INVESTIGATION OF DRAG REDUCTION
BY BOUNDARY-LAYER SUCTION
ON A 50-DEG SWEPT TAPERED WING
AT M_∞ = 2.5 TO 4

By

S. R. Pate

von Kármán Gas Dynamics Facility

ARO, Inc.

TECHNICAL DOCUMENTARY REPORT NO. AEDC-TDR-64-221

October 1964

Program Element 62405334/1366, Task 136612

ARNOLD ENGINEERING DEVELOPMENT CENTER

AIR FORCE SYSTEMS COMMAND

UNITED STATES AIR FORCE

NOTICES

INVESTIGATION OF DRAG REDUCTION

BY BOUNDARY-LAYER SUCTION

ON A 50-DEG SWEPT TAPERED WING

AT M_∞ = 2.5 TO 4

By

S. R. Pate

von Kármán Gas Dynamics Facility

ARO, Inc.

a subsidiary of Sverdrup and Parcel, Inc.

October 1964

ARO Project No. VA0446

ABSTRACT

Tests were conducted in the 40-in. supersonic Tunnel A of the von Kármán Gas Dynamics Facility to determine the effectiveness of boundary-layer suction for laminar flow control on a tapered, three-dimensional, 50-deg swept supersonic wing. Test Mach numbers were 2.5, 3, 3.5, and 4 with a Reynolds number range (based on boundary-layer rake location) from 4.3 to 19.5 million for angles of attack of zero and ±3 deg.

With suction, full-chord laminar flow was maintained for small angles of attack at M_∞ = 2.5, 3, and 3.5 up to length Reynolds numbers of 17, 12, and 9 million, respectively. Wake drag, suction drag, and total drag coefficients and the corresponding suction coefficients are presented, along with fully turbulent wake drag coefficients for the no-suction case.

PUBLICATION REVIEW

This report has been reviewed and publication is approved.

Darreld K. Calkins
Major, USAF
AF Representative, VKF
DCS/Test

Jean A. Jack
Colonel, USAF
DCS/Test

CONTENTS

ILLUSTRATIONS

NOMENCLATURE

A_n	Reference area based on n^{th} chamber average span and rake location $(A_n = b_n \cdot x)$, sq in.
b_n	Reference width (average span, n^{th} chamber), in.
C_{DS}	Suction drag coefficient
C_{DT}	Total drag coefficient, $(C_{DW} + C_{DS})$
C_{DW}	Wake drag coefficient, $(2\theta_\infty/x)$
C_{m_η}	Local suction coefficient, $(m_n/\rho_\infty U_\infty A_n)$
C_{mt}	Total suction coefficient, $\sum\limits_{n=1}^{x} C_{m_n}$
c	Wing chord, in.
LE	Leading edge
M_n	Suction chamber Mach number
M_r	Mach number outside the boundary layer
M_∞	Free-stream Mach number
m_n	Local mass rate of suction, lb-sec/in.
p	Model surface pressure, psia
p_∞	Free-stream static pressure, psia
q_∞	Free-stream dynamic pressure, psia
Re	Reynolds number
Re_x	Reynolds number based on rake location
T_n	Suction chamber temperature, °R
T_∞	Free-stream static temperature, °R
U_r	Velocity outside boundary layer, in./sec
U_∞	Free-stream velocity, in./sec
u	Local velocity in boundary layer, in./sec
x	Boundary-layer rake location, measured from model leading edge, in.
y	Distance normal to model surface, in.
α	Wing angle of attack, deg

δ — Boundary-layer total thickness, in.

θ_r — Boundary-layer momentum thickness at rake location, in.

$$\int_{o}^{\delta} \frac{\rho\,u}{\rho_r\,U_r}\left(1 - \frac{u}{U_r}\right) dy$$

θ_∞ — Boundary-layer momentum thickness for free-stream conditions, in.

ρ — Local density in boundary layer, $\dfrac{\text{lb-sec}^2}{\text{in.}^4}$

ρ_r — Density outside boundary layer, $\dfrac{\text{lb-sec}^2}{\text{in.}^4}$

ρ_∞ — Free-stream density, $\dfrac{\text{lb-sec}^2}{\text{in.}^4}$

SUBSCRIPTS

n — The nth suction chamber

r — Conditions outside the boundary layer

∞ — Free-stream conditions

1.0 INTRODUCTION

At the request of the Air Force Flight Dynamics Laboratory (AFFDL), Air Force Systems Command (AFSC), a boundary-layer laminar flow control test was conducted on a three-dimensional, tapered, 50-deg swept wing for the NORAIR Division of the Northrop Corporation. Tests were made in the Gas Dynamic Wind Tunnel, Supersonic (A) of the von Kármán Gas Dynamics Facility (VKF), Arnold Engineering Development Center (AEDC), AFSC, during the period of July 13-25, 1964. Test Mach numbers were 2.5, 3, 3.5, and 4 over a Reynolds number range, based on rake location, from 4.3 to 19.5 million at angles of attack of 0 and ±3 deg.

The purpose of the test was to determine if full-chord laminar flow could be established at high Reynolds numbers with boundary-layer suction on a highly swept, three-dimensional, tapered, supersonic wing, and to measure the suction requirements and wake drag.

2.0 APPARATUS

2.1 WIND TUNNEL

Tunnel A (Fig. 1) is a continuous, closed-circuit, variable density wind tunnel with an automatically driven flexible-plate-type nozzle and a 40- by 40-in. test section. The tunnel operates at Mach numbers from 1.5 to 6 at maximum stagnation pressures from 29 to 200 psia, respectively, and stagnation temperatures up to 300°F (M_∞ = 6). Minimum operating pressures are about one-tenth of the maximum at each Mach number. A description of the tunnel and airflow calibration information may be found in Ref. 1.

2.2 MODEL

The NORAIR 50-deg swept, tapered wing (Fig. 2a) spanned the tunnel test section and was supported by the tunnel sidewalls. The wing (Fig. 3) had a 2.5-percent-thick biconvex (in flow direction) airfoil section with a LE thickness of 0.005 in. A section of the top surface was vented with 67 suction slots (0.007- to 0.010-in. in width) through

---

Manuscript received September 1964.

which a portion of the boundary layer was removed (see Fig. 3). A detachable end plate, as shown in Fig. 4, was employed to determine if the three-dimensional pressure field emanating from the wing-wall or wing-plate junction was critical in establishing laminar flow.

Eleven separate suction chambers were contained within the model and connected separately to individual metering boxes; thus variable suction was provided over the model surface. The model was instrumented to measure the surface pressure along three spanwise stations (see Fig. 4), and ambient pressure was measured in each of the eleven suction chambers. Temperatures were measured at five chordwise stations and in five of the eleven suction chambers.

2.3 BOUNDARY-LAYER RAKE

The rake (Fig. 5) was composed of 10 probes ranging in height (distance from probe centerline to model surface) from 0.015 to 0.340 in. Each probe had an ID of 0.010 in. and an OD of 0.012 in. at the tip and was located in a plane parallel to the last suction slot. The probes could be automatically driven to traverse a distance of 11 in. (from the trailing edge) along the wing span station located 16.8 in. from the wing root as shown in Fig. 4. A magnet was located in the probe head to ensure continuous contact with the curved surface.

2.4 SUCTION SYSTEM

Suction (operating range from 0.04 to 0.14 psia) was provided by a 12-in. vacuum line, which was connected separately by 2-in.-ID rubber pipe to each of the eleven metering boxes (Figs. 2b and 6). Flow regulation to each suction chamber was maintained by a throttling valve on each metering box. Calibrated nozzles facilitated measurement of the different levels of mass flow from each of the eleven suction chambers.

2.5 INSTRUMENTATION

Model data recorded during the test were boundary-layer pitot pressures, model surface static pressures, suction chamber ambient pressures and temperatures, metering chamber total pressure and temperatures, and metering nozzle static pressures. All model and rake pressures were measured with the standard Tunnel A pressure-scanning system using 1- and 15-psid transducers referenced to a near vacuum. The 15-psid transducers were calibrated for ranges of 18, 6, and 2.5 psia, and the 1-psid transducers were calibrated for

ranges of 1, 0.5, and 0.25 psia. The precision of the system is esti-
mated to be within one percent of the range being used. The metering
chamber pressures and nozzle pressures were measured with 1- and
5-psid transducers referenced to a near vacuum, which are considered
accurate to within about 0.2 percent of the transducer capacity. Data
were processed with the VKF data-handling system and computer to
provide reduced data while the test was in progress.
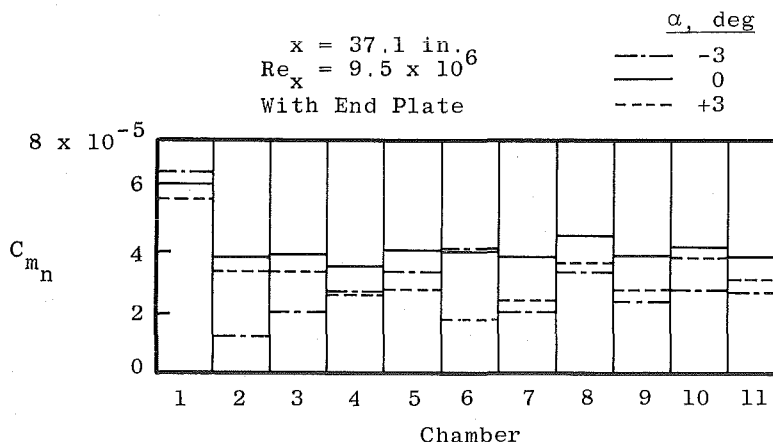
3.0 PROCEDURE

Testing was conducted with variable suction and no suction, with
and without end plate, over the following range of test conditions:

Nominal Mach No.	Maximum Re/in. x 10^{-6}	Minimum Re/in. x 10^{-6}	Rake Location, in.	α, deg
2.5	0.53	0.24	37.1 to 26.1	-3, 0, +3
3.0	0.43	0.19	37.1 to 26.1	-3, 0, +3
3.5	0.51	0.14	37.1 to 26.1	-3, 0, +3
4.0*	0.19	0.15	37.1 to 28.8	-3

*Without End Plate Only

Boundary-layer pitot pressure profiles were measured for the
above-listed test conditions. The condition of no suction was obtained
by closing the metering chamber valves and leaving the slots unsealed.
The effect of varying the suction quantities through the eleven chambers
was observed by noting the changes in the boundary-layer pitot pressure
profile at a particular rake station.

The following chart shows a typical suction coefficient distribution
for the cases of optimum suction (lowest total drag) at one Reynolds
number and at angles of attack of -3, 0, and +3 deg for Macn number 3.

$$x = 37.1 \text{ in.}$$
$$Re_x = 9.5 \times 10^6$$
With End Plate

	α, deg
—·—	-3
——	0
----	+3

C_{m_n}

Chamber

4.0 DATA ANALYSIS

Reduction of the boundary-layer data consisted of determining the momentum thickness from a graphical integration of the momentum parameter. The momentum parameter was normalized with respect to the local free-stream conditions ($\rho_r U_r$), which were determined from the measured local static pressure on the model surface and the tunnel stagnation conditions. The loss in total pressure attributable to the model leading-edge shock and the suction slot shocks was considered to be negligible.

For a surface with zero pressure gradient ($U_r = U_\infty$) the wake drag coefficient, which is the skin friction coefficient per unit span, is determined from

$$C_{D_W} = \frac{2\theta_\infty}{x} = \frac{2\theta_r}{x} \tag{1}$$

where x is the distance of the boundary-layer rake from the model leading edge. If the conditions outside the boundary layer at the rake location differ from free stream ($U_r \neq U_\infty$) and the momentum equation of the wake is solved, then the wake drag coefficient (composed of skin friction and form drag) can be expressed as shown in Ref. 2 by

$$C_{D_W} = \left(\frac{2\theta_r}{x}\right)\left(\frac{U_r}{U_\infty}\right)^{3.145 - 0.28\,M_r^2 - 0.30\,M_\infty^2} \tag{2}$$

In the following table are given the wake drag coefficients as determined by the two methods, Eqs. (1) and (2):

M_∞	a, deg	Re_x x 10^{-6}	θ_r x 10^3	Eq. (1) $C_{D_W} = \frac{2\theta_r}{x}$ x 10^3	Eq. (2) $C_{D_W} = \left(\frac{2\theta_r}{x}\right)\left(\frac{U_r}{U_\infty}\right)^{(3.145 - 0.28\,M_r^2 - 0.30\,M_\infty^2)}$ x 10^3
2.5	+3	15.40	5.572	0.3004	0.2905
3.0	-3	9.43	7.972	0.4298	0.4298
3.0	0	9.53	4.188	0.2257	0.2197
3.0	+3	9.61	5.940	0.3202	0.2981
3.5	-3	8.95	5.372	0.2896	0.2884
3.5	0	9.05	7.564	0.4078	0.3878

x = 37.1 in.   With End Plate

Differences up to approximately seven percent existed, and therefore all data presented in this report were determined by Eq. (2).

The suction coefficient per unit span is defined by

$$C_{m_t} = \sum_{n=1}^{x} C_{m_n} = \sum_{n=1}^{x} \frac{m_n}{\rho_\infty U_\infty A_n} \tag{3}$$

Consideration of the reduction in skin friction drag by using suction must necessarily include an evaluation of the penalties in drag caused by suction. The total drag coefficient (C_{D_T}) then consists of a summation of the wake drag and suction drag coefficients ($C_{D_T} = C_{D_W} + C_{D_S}$).

The suction drag coefficient is determined by the power required to accelerate the air removed from the boundary layer to free-stream conditions and is based on the assumption that the flow is isentropic and the efficiency of the suction compressor is equal to the propulsive efficiency of the propulsion system. The suction drag coefficient can then be expressed as shown in Ref. 2 by

$$C_{D_S} = \sum_{n=1}^{x} (C_{D_S})_n = \sum_{n=1}^{x} C_{m_n}\left(1 + \frac{M_n^2 T_n}{M_\infty^2 T_\infty}\right) \tag{4}$$

When the wing is at an angle of attack, and the pressure on the suction area surface is not equal to the zero angle-of-attack condition, then the suction drag requirements, as computed by Eq. (4), must be corrected by the ratio $(\rho_\infty U_\infty)/(\rho_r U_r)$, where $\rho_r U_r$ are the conditions at the 50-percent chord.

Then for angle of attack

$$C_{D_S} = \sum_{n=1}^{x} (C_{D_S})_n \left(\frac{\rho_\infty U_\infty}{\rho_r U_r}\right) = \sum_{n=1}^{x} C_{m_n}\left(\frac{\rho_\infty U_\infty}{\rho_r U_r}\right)\left(1 + \frac{M_n^2 T_n}{M_\infty^2 T_\infty}\right) \tag{5}$$

The suction coefficient at angle of attack is also presented as

$$C_{m_t} = \sum_{n=1}^{x} C_{m_n}\left(\frac{\rho_\infty U_\infty}{\rho_r U_r}\right) = \sum_{n=1}^{x} \frac{m_n}{\rho_r U_r A_n} \tag{6}$$

where $\rho_r U_r$ are values at the 50-percent chord.

At Mach numbers 2.5, 3, and 3.5, the ratio $(\rho_\infty U_\infty)/(\rho_r U_r)$ for $\alpha = -3$ and $+3$ deg are listed in the following table:

M_∞	α, deg	$(\rho_\infty U_\infty)/(\rho_r U_r)$	α, deg	$(\rho_\infty U_\infty)/(\rho_r U_r)$
2.5	-3	0.87	+3	1.16
3.0	-3	0.86	+3	1.18
3.5	-3	0.85	+3	1.19

(At $\alpha = 0$, $(\rho_\infty U_\infty)/(\rho_r U_r) = 1$)

5

An alternate procedure available for evaluating the suction drag consists of assuming that all the momentum removed from the boundary layer is lost, and the drag coefficient thus determined is

$$C_{D_S} = \sum_{n=1}^{x} \frac{\text{suction drag}}{q_\infty A_n} = \sum_{n=1}^{x} \frac{m_n U_\infty}{\frac{1}{2} \rho_\infty U_\infty^2 A_n} = 2 \sum_{n=1}^{x} C_{m_n} \qquad (7)$$

These two methods determine the limits on suction drag. Shown below are the suction drag coefficients applied to typical data and the total drag coefficients for the two methods of evaluating suction drag:

M_∞	α, deg	Re_x x 10^{-6}	C_{D_W} x 10^3	C_{D_S} x 10^3	$C_{D_T} = \left(C_{D_W} + C_{D_S}\right) \times 10^3$
3.0	0	9.53	0.2197	Eq. (4): 0.5147	0.7344
3.0	0	9.53	0.2197	Eq. (7): 0.9478	1.168

x = 37.1 in.   With End Plate

All suction drag coefficients used in this report were determined from the relationships expressed in Eqs. (4) and (5).

5.0 RESULTS AND DISCUSSION

Presented in Fig. 7 are the wing surface pressure data obtained with and without the end plate for α = -3, 0, and +3 deg and M_∞ = 3. For α = -3 and 0 deg the presence of the end plate produced an expansion flow field and the result was a significant decrease in the surface pressures aft of the Mach line emanating from the wing-plate junction. The effect of the disturbances resulting from the wing-wall or wing-plate junction can also be seen by comparing the data for the three different spanwise stations and noting from the sketch where the Mach line crosses the wing surface. At α = +3 deg the pressure data indicate that disturbances from the wing-wall or wing-plate junction were insignificant. Whether the three-dimensional flow field resulting from a wing-end plate configuration is a compression or expansion flow field will depend on model surface geometry and model attitude.

Presented in Fig. 8 are typical boundary-layer profiles for Mach numbers 2.5, 3, 3.5, and 4 at α = -3, 0, and +3 deg for x = 28.8 and 37.1 in. with conditions of suction and no suction. As seen from these figures, suction was adequate to establish laminar flow at all test Mach

numbers except Mach number 4. The laminar profiles are for the optimum suction condition (lowest total drag) and the turbulent profiles for the conditions of no suction and the slots unsealed.

As suction is increased, the wake drag will decrease, the suction drag increase, and therefore a minimum value for the total drag will exist for a particular suction quantity which will be the optimum. Minimum total drag and optimum suction coefficients are presented in Fig. 9, along with wake drag and suction drag coefficients, for M_∞ = 2.5, 3, 3.5, and 4 for various Reynolds numbers. For M_∞ = 2.5 (Fig. 9a) full-chord (x = 37.1 in.) laminar flow was maintained up to approximately Re_x = 17 x 10^6 for α = +3 deg and up to approximately Re_x = 7 x 10^6 for α = -3 and 0 deg. Maintaining laminar flow at α = -3 and 0 deg at this Mach number was restricted by the leading-edge shock which reflected from the tunnel walls and impinged on the model surface, crossing the suction area centerline at x/c values of approximately 48 and 65 percent, respectively.

At M_∞ = 3 (Fig. 9b) full-chord (x = 37.1 in.) laminar flow was maintained up to $Re_x \approx$ 12 x 10^6 for α = 0 and $Re_x \approx$ 10 x 10^6 for α = -3 and +3 deg. For M_∞ = 3.5 (Fig. 9c) full-chord laminar flow was maintained up to $Re_x \approx$ 9 x 10^6 for α = -3 and 0 deg. At α = +3 deg (Fig. 9c) the total drag coefficient (C_{D_T}) was considerably less than the no-suction, fully turbulent drag values because of the thinning of the boundary layer, but laminar flow was not established as is evidenced by comparing the wake drag coefficients for α = -3 and +3 deg. The significance of wing angle of attack can be explained by the substantial increase in the inviscid Mach number (M_r) at the rake location for α = +3 deg where M_r was 3.85 as compared to M_r = 3.49 for α = -3 deg. The model suction slots were designed primarily for the range M_∞ = 3 to 3.5, and consequently the suction was inadequate at the higher Mach numbers.

At M_∞ = 4 (Fig. 9d) laminar flow was not established for α = -3 deg, x = 37.1 in. The surface Mach number at the rake location (M_r) was 3.92, and these data agreed fairly well with the M_∞ = 3.5 data for α = +3 deg where M_r = 3.85.
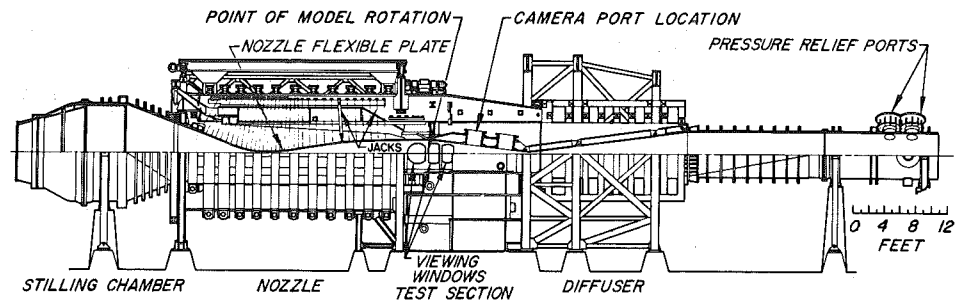
6.0 CONCLUDING REMARKS

Tests were conducted at Mach numbers 2.5, 3, 3.5, and 4 to determine the effectiveness of boundary-layer suction for laminar flow

control on a tapered, 50-deg, swept wing. On the basis of these tests the following conclusions are made:
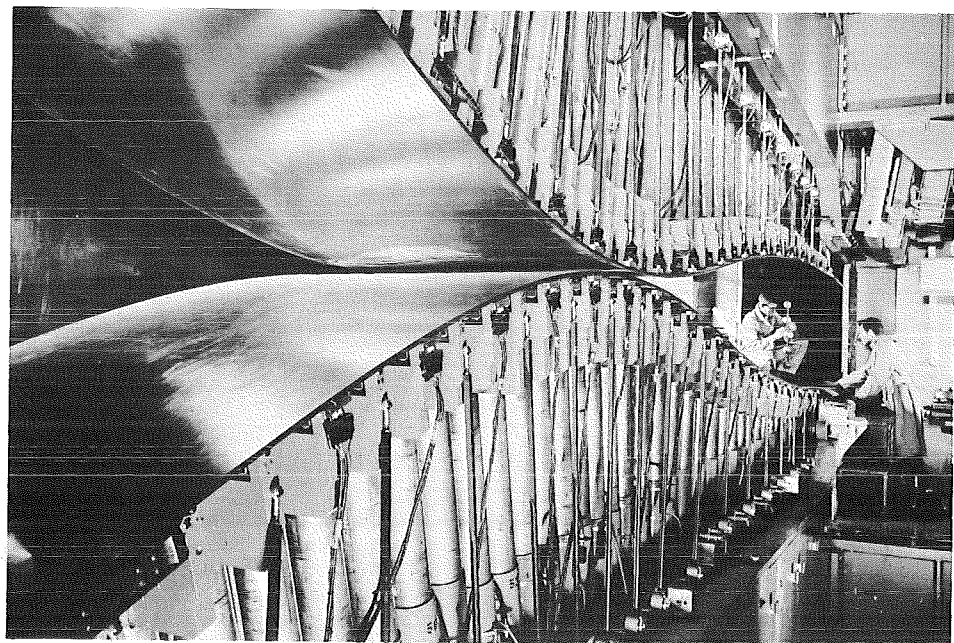
1. Full-chord laminar flow was established at M_∞ = 2.5, 3, and 3.5 up to Reynolds numbers, based on rake location, of approximately 17, 12, and 9 million, respectively.

2. Laminar flow was not established when the local outer flow Mach number (M_r) at the rake location was appreciably higher than the suction design Mach number of 3.5.

REFERENCES

1. Coats, Jack D. "Flow Characteristics of a 40-Inch Wind Tunnel at Mach Numbers 1.5 to 6." AEDC-TDR-62-130 (AD 277289), June 1962.

2. Groth, E. "Boundary Layer Suction Experiments at Supersonic Speeds." Boundary Layer and Flow Control edited by Lachmann, G. V., Vol. 2, Pergamon Press, New York, Oxford, London, Paris, 1961.

3. Van Driest, E. R. "Turbulent Boundary Layer in Compressible Fluids." Journal of the Aeronautical Sciences, Vol. 18, No. 3, March 1951, pp. 145-160, 216.
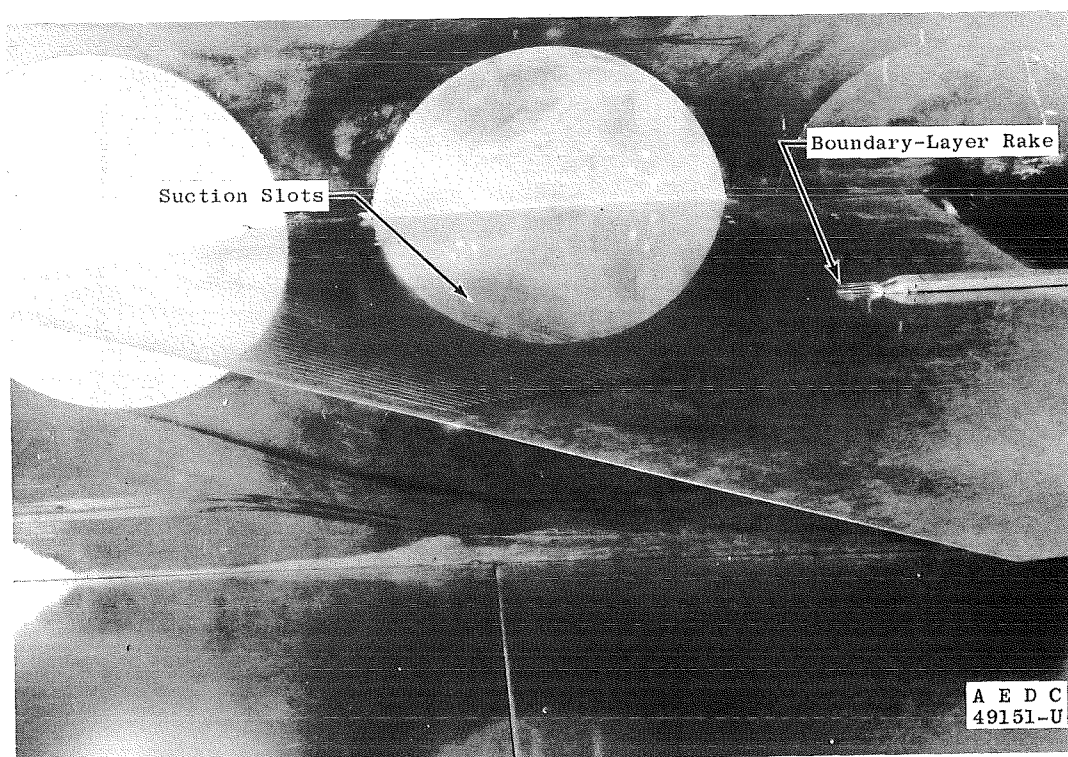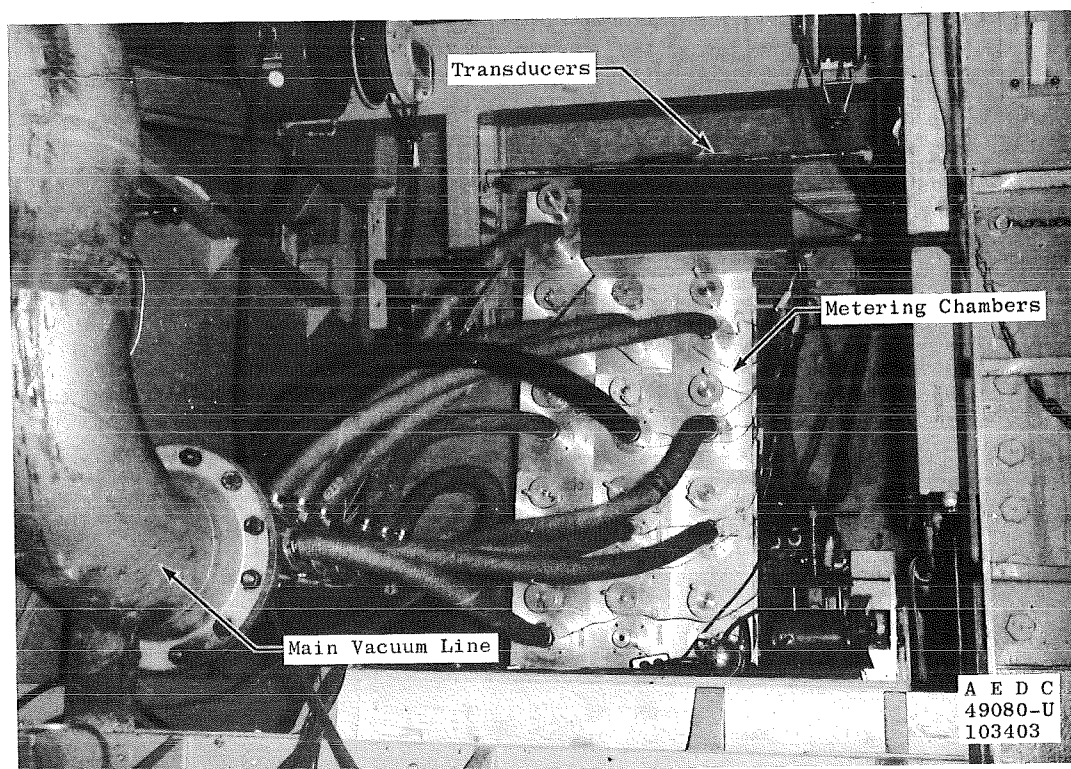
Assembly

Nozzle and Test Section

Fig. 1 Tunnel A

Suction Slots

Boundary-Layer Rake

A E D C
49151-U

a. Model Installation

Transducers

Metering Chambers

Main Vacuum Line

A E D C
49080-U
103403

b. Suction Equipment

Fig. 2 Model Installation and Suction Equipment

Instrumentation Exit

Suction Chamber
Connection Lines (11 Places)

Tunnel Wall

58.0

13.6 16.8

Suction Slots (67 Total)

9.3

22.5

1.30

Flow

40.4

A

A

Rake Location

1.00

40.0

0.72

0.005

50 deg

6 deg

Tunnel Wall

12 deg

Chamber
No. 1 2 3

10.3

View B

B

All Dimensions in Inches

4 5 6 7 8 9 10 11 2.1

Section AA

Suction Slot Locations and Dimensions		
Chamber No.	Slot No.	Slot Width, in.
1	1-6	0.007
2	7-11	0.008
3	12-16	0.008
4	17-21	0.009
5	22-26	0.010
6	27-32	
7	33-38	
8	39-45	
9	46-52	
10	53-59	
11	60-67	0.009

103404

Fig. 3 Model Geometry

Pressure Orifice Location		Thermocouple Locations		
No.	Percent Chord	No.	Percent Chord	Spanwise Location, in.
1	14.7	1	20.6	18.75
2	15.1	2	36.4	18.75
3,4	29.1	3	51.9	18.75
5,6,7	43.5	4	71.5	18.75
8,9,10	63.1	5	90.3	18.75
11	74.3	6	Chamber No. 2	
12	84.5	7	Chamber No. 4	
13	96.1	8	Chamber No. 6	
14-24	One in Each Chamber	9	Chamber No. 8	
		10	Chamber No. 10	

All dimensions are in inches.

103405

Fig. 4 Sketch of Model with Attached End Plate

At LE {0.010 ID
{0.012 OD

0.50

0.20

0.020 OD

0.042 OD

View A

Probe Detail

Probe No.	y, in.
1	0.015
2	0.025
3	0.040
4	0.060
5	0.085
6	0.115
7	0.150
8	0.205
9	0.265
10	0.340

6 deg

2.00

0.20

¢

0.15

Plan View

Magnetic Head

Roll Pin

A

y

0.340

Model Surface

All dimensions are in inches.

Side View
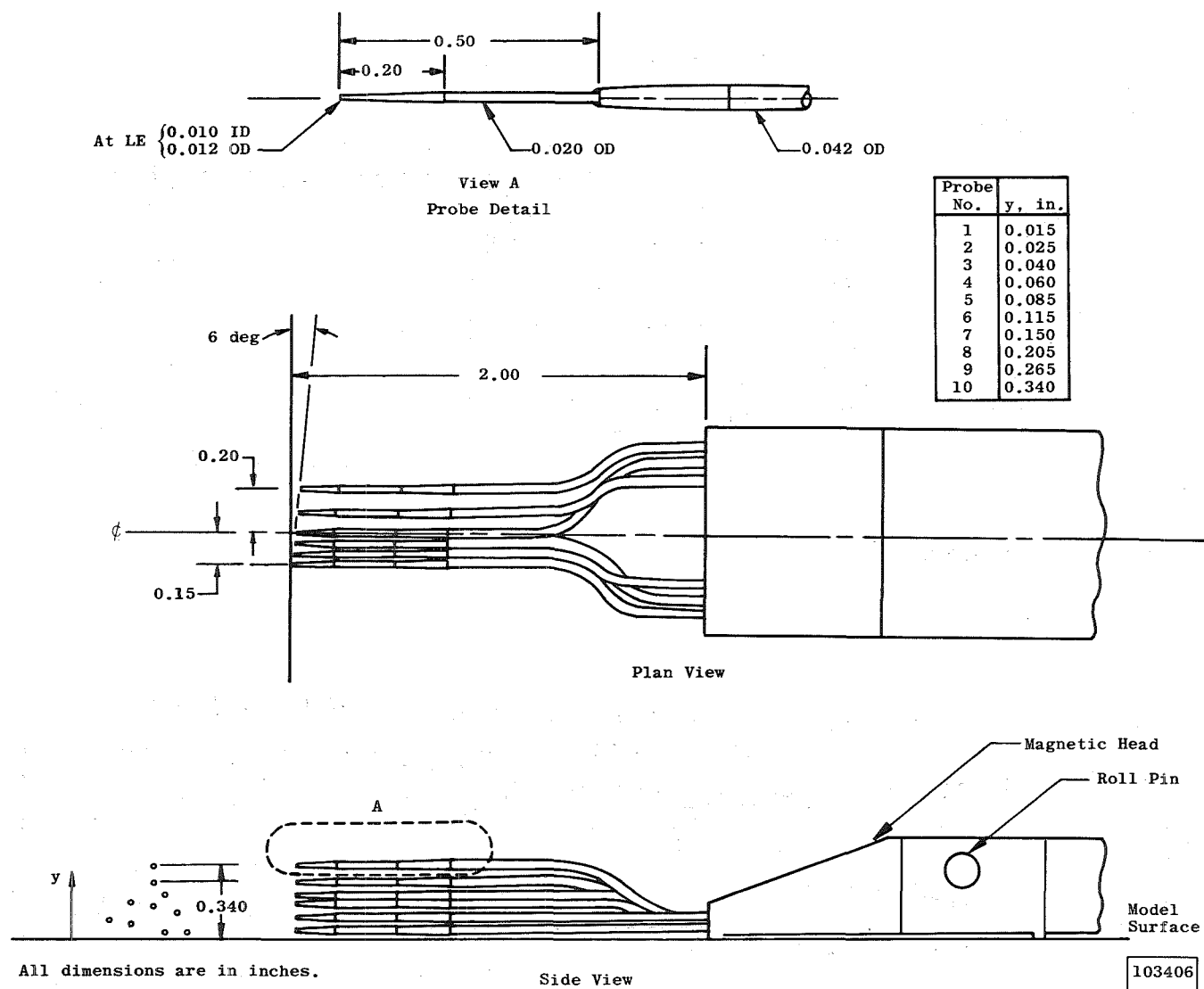
103406

Fig. 5 Sketch of Boundary-Layer Rake
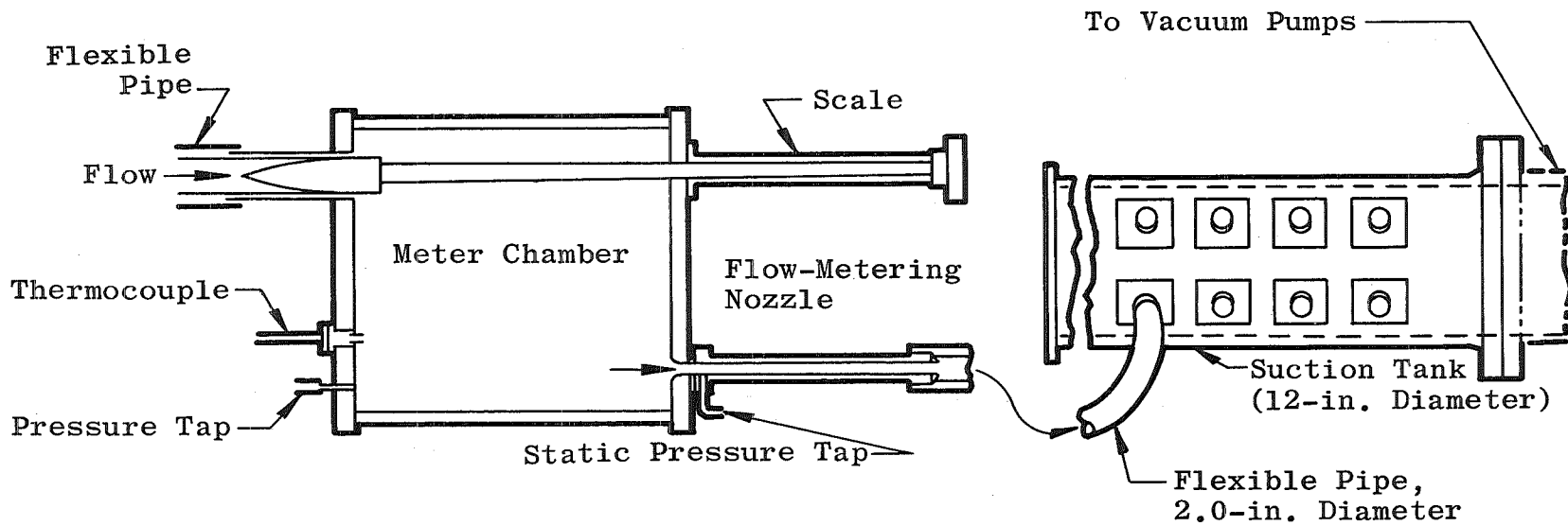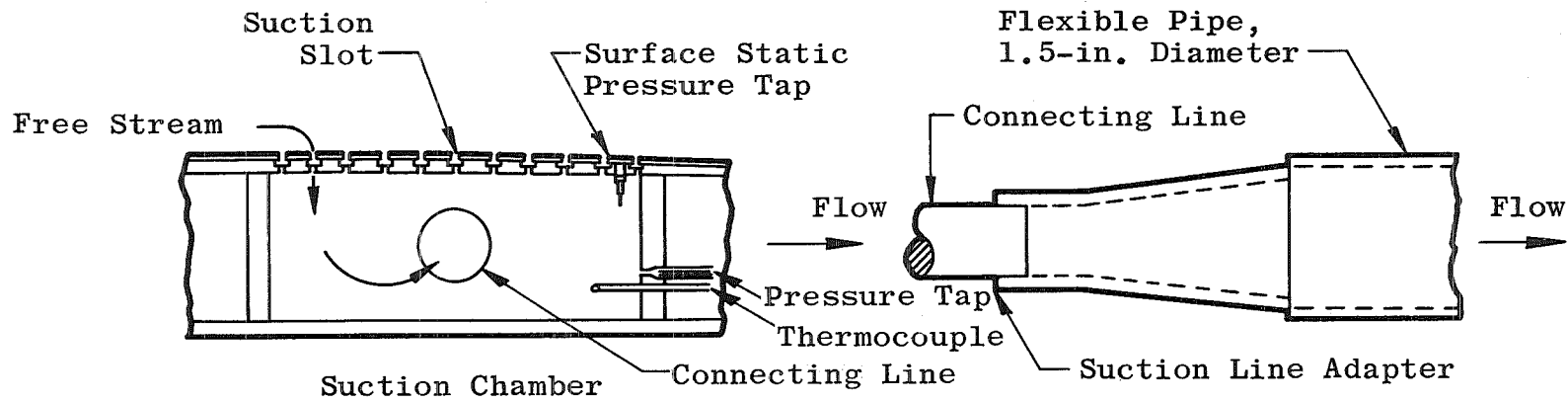
Fig. 6 Schematic Drawing of Suction System

103407
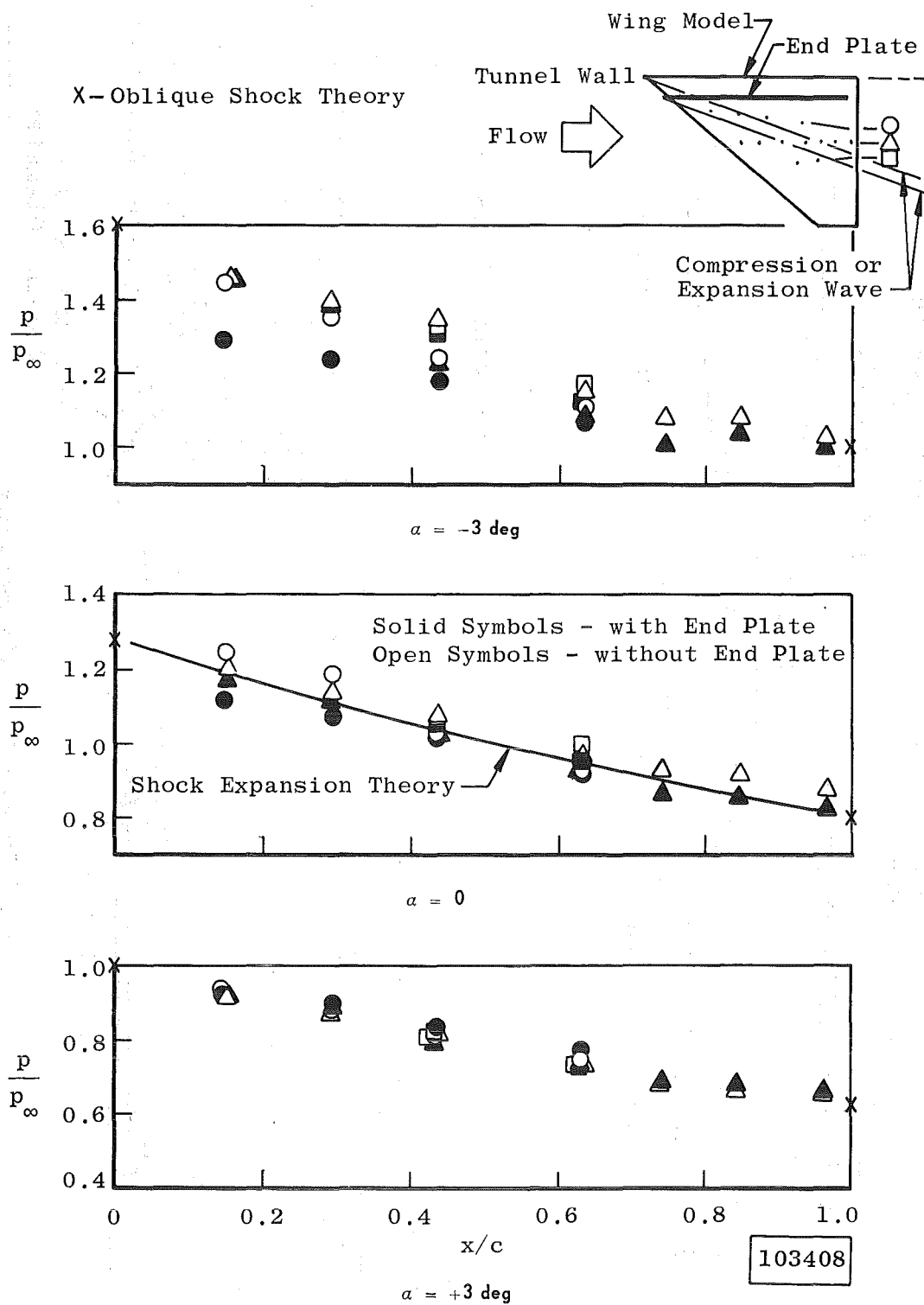
Fig. 7 Wing Surface Pressure Distribution for $\alpha = -3$, 0, and +3 deg for $M_\infty = 3$

15

Velocity Profiles

Momentum Profiles
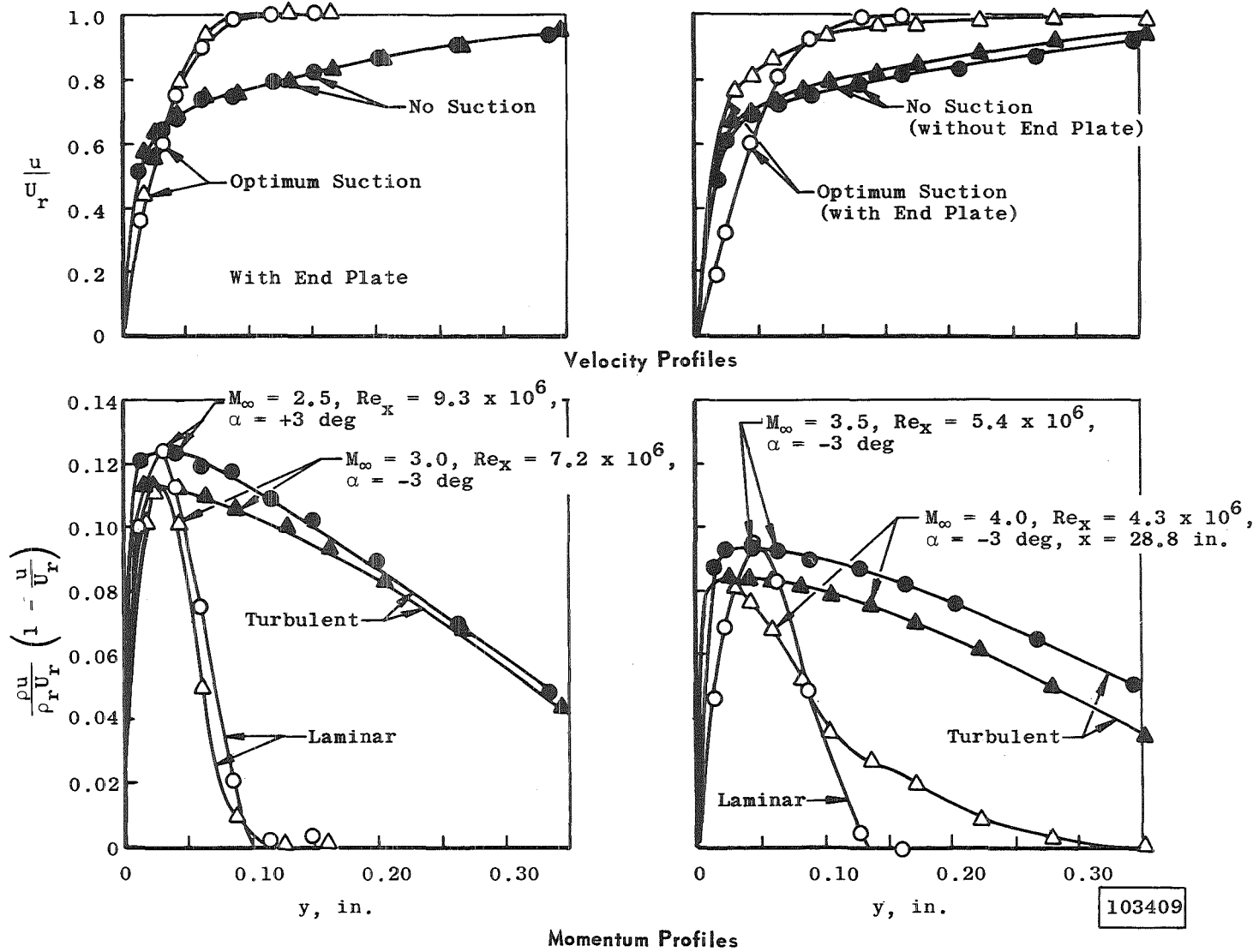
Fig. 8 Boundary-Layer Profiles at Station x = 37.1 in. for α = −3, 0, and +3 deg with and without Suction
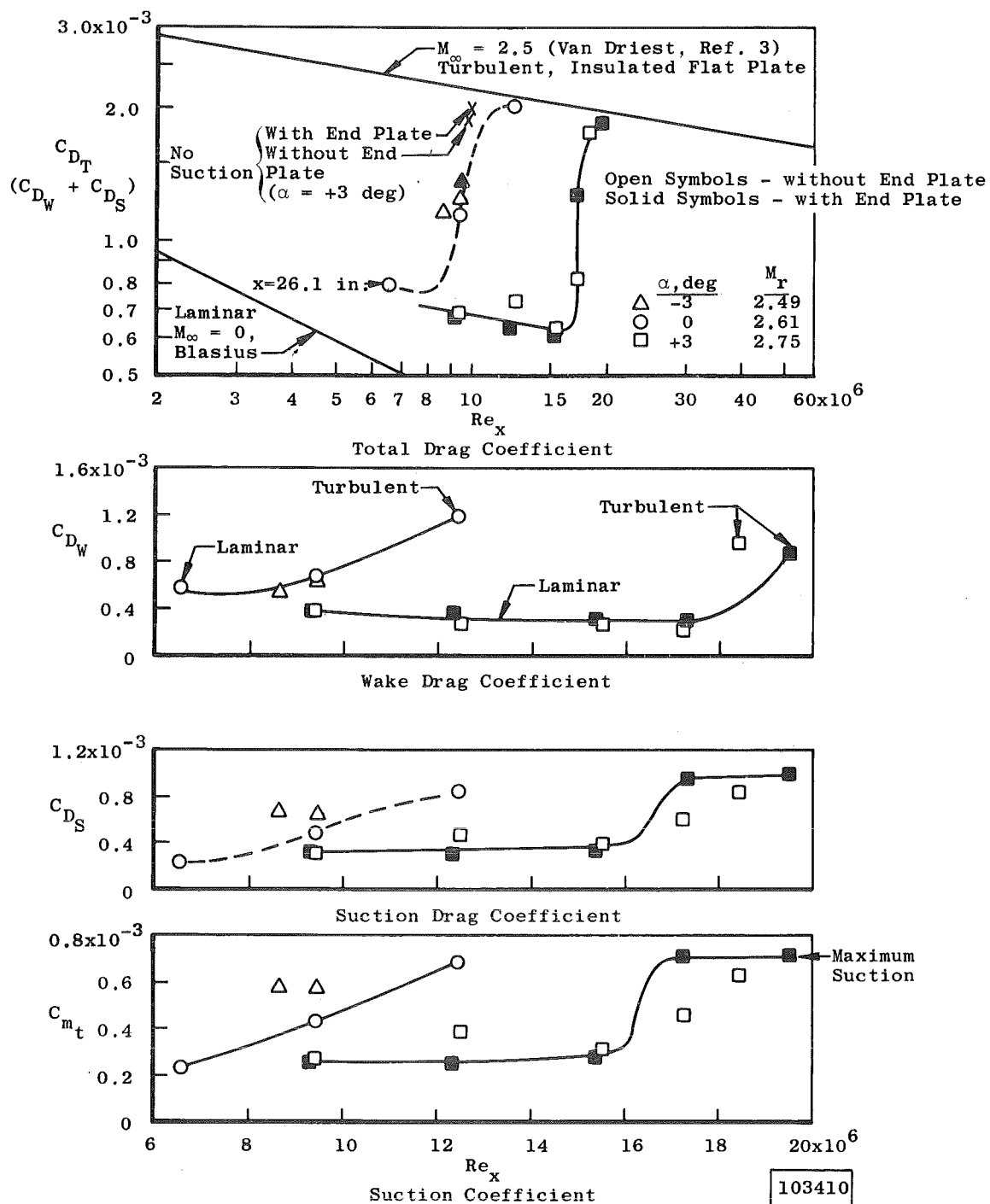
a. $M_\infty = 2.5$

Fig. 9 Drag and Suction Coefficients versus Reynolds Number at
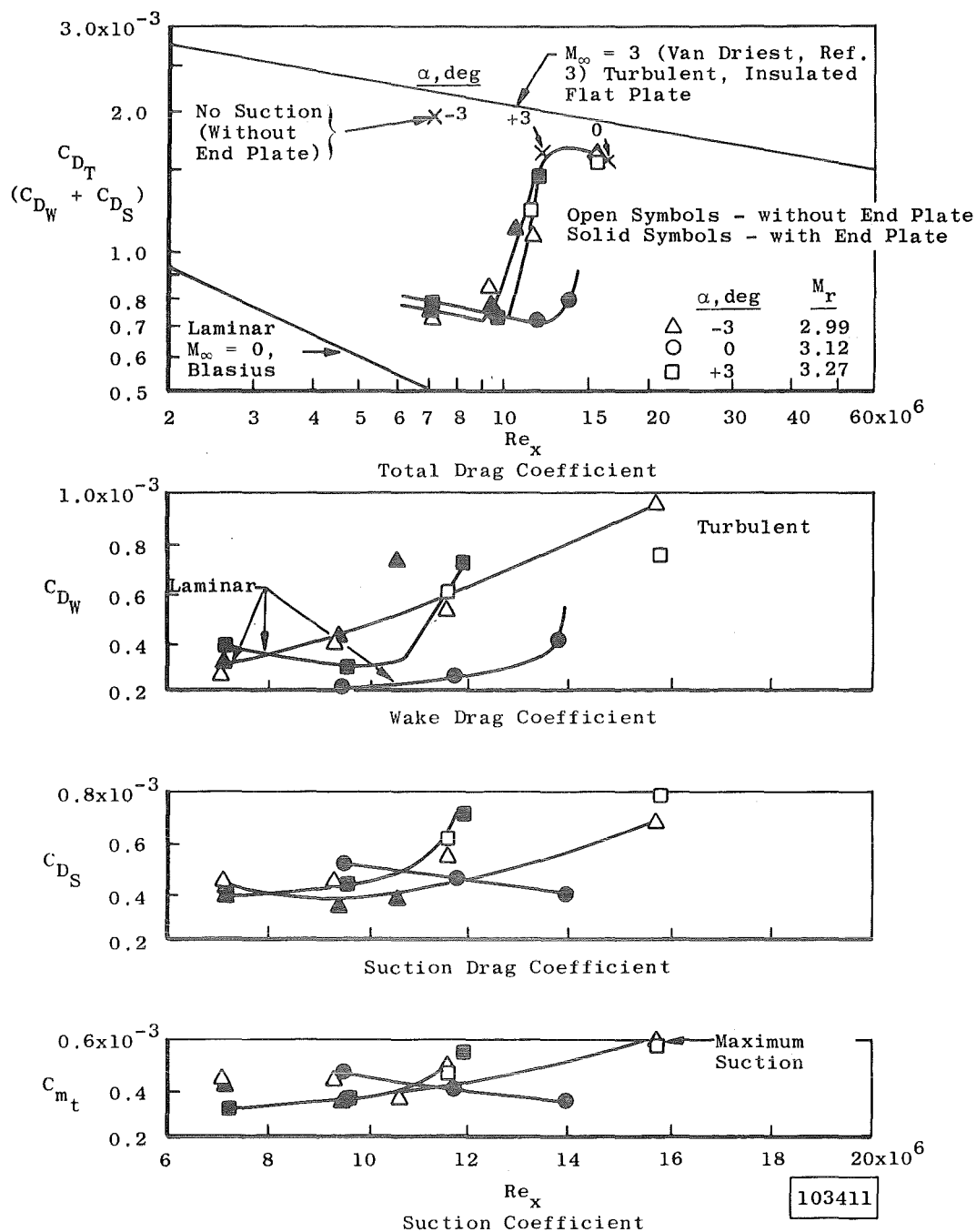Station x = 37.1 in. for α = −3, 0, and +3 deg and
M_∞ = 2.5, 3, 3.5, and 4
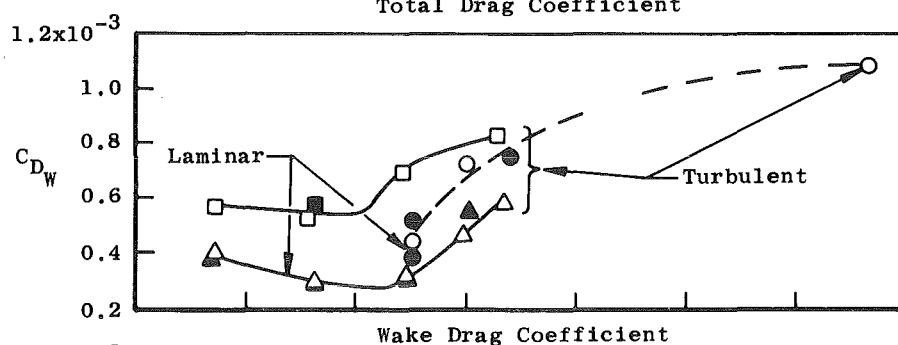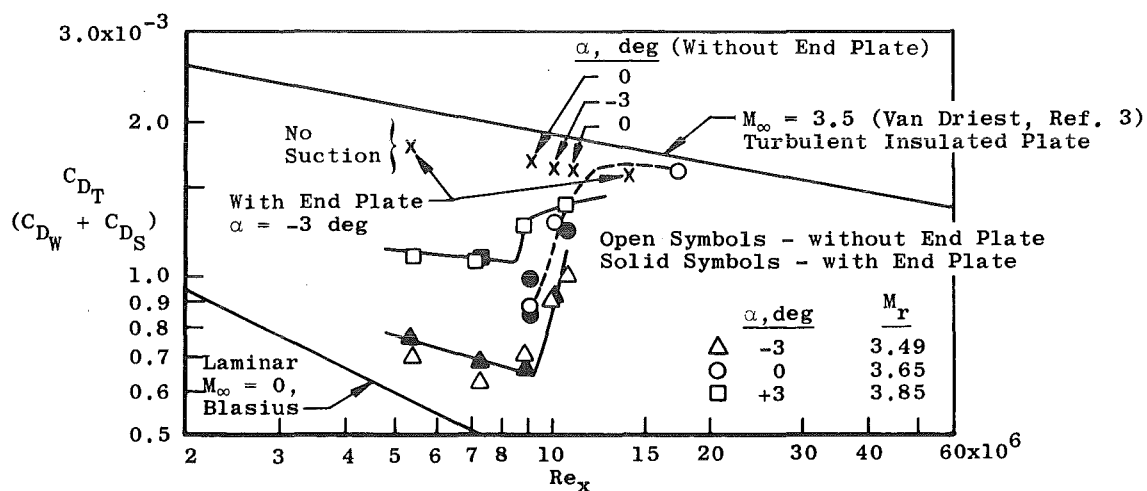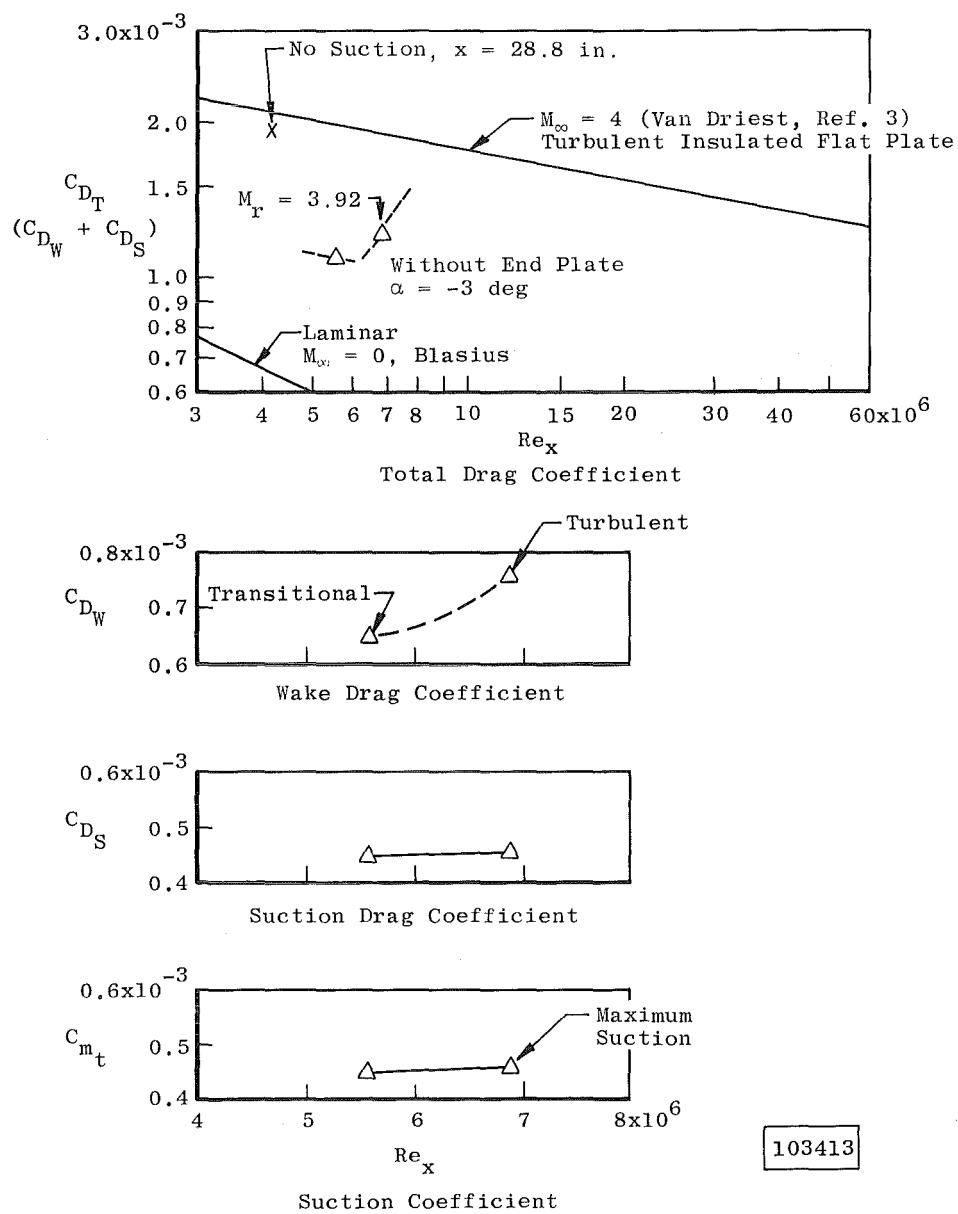
17

b. $M_\infty = 3$

Fig. 9 Continued

18

c. $M_\infty = 3.5$

Fig. 9 Continued

19

d. $M_\infty = 4$

Fig. 9 Concluded